*Journal of Applied Pharmaceutical Research*
*Volume 13 Issue 2, Year of Publication 2025, Page 73 – 85*
*DOI: https://doi.org/10.69857/joapr.v13i2.1006*

Check for updates

**Research Article**

***JOURNAL OF APPLIED PHARMACEUTICAL RESEARCH | JOAPR***
***www.japtronline.com*** ***ISSN: 2348 – 0335***

# *CHITOSAN-COATED CMC AND CARBOPOL HYDROGEL BEADS FOR CONTROLLED RELEASE OF METFORMIN IN DIABETES MANAGEMENT*

Sachin Gupta[1,2], Swati Dubey[2], Sanjeev Kumar Patel[2], Anshu Priyanka Lakra[3], Sunita Minz[2]*

***Article Information***
Received: 16th December 2024
Revised: 28th March 2025
Accepted: 13th April 2025
Published: 30th April 2025

**Keywords**
*Metformin HCl, beads, Diabetes Mellitus, chitosan, carboxymethyl cellulose sodium, carbopol.*

***ABSTRACT***

**Background:** Current research aims to fabricate carboxymethyl cellulose sodium (CMC-Na) and carbopol hydrogel beads. Gleichzeitig, beads were coated with chitosan to enhance the controlled release of the drug Metformin HCl (MET), which serves as a model drug for diabetes mellitus (DM). **Methodology:** The MET beads were synthesized through the ionotropic gelation process. The foundation of ionotropic gelation is a polyelectrolyte's capacity to cross-link to create hydrogels when counterions are present. The negatively charged carboxylate groups ($-COO^-$) on CMC-Na form electrostatic interactions with the positively charged aluminium ions ($Al^{3+}$) from $AlCl_3$. The quality-by-design approach was employed to optimize process factors in preparing hydrogel beads. A comprehensive evaluation of the beads covered various aspects such as particle size, scanning electron microscopy, percentage yield, Fourier transform infrared spectroscopy, X-ray diffraction, entrapment efficiency (EE), and *in vitro* drug release. **Results and Discussion:** The beads were spherical, with an average particle diameter of 153.6 to 231.5 µm. The entrapment efficiency percentage range is 94.4% and 97.83% for MET-loaded and chitosan-coated MET-loaded beads, respectively. Therefore, *in-vitro* drug release of the optimized MET-loaded beads is 55.5 %, and chitosan-coated MET-loaded beads are approximately 48.8% achieved in 10 hours. **Conclusion:** Chitosan-coated CMC-Na and carbopol hydrogel beads showed good MET encapsulation and sustained release, improving structural integrity and drug release. The ionotropic gelation process created stable, homogeneous beads, making this delivery method viable for oral sustained-release MET formulations.

## *INTRODUCTION*

Approximately 10% of the global population is affected by diabetes mellitus (DM), a prevalent metabolic disorder marked by chronic hyperglycemia and whose incidence is expected to rise in the coming years [1]. Particles with a size greater than 10 µm struggle to penetrate the mucus layer of the gastrointestinal tract (GIT) effectively. Therefore, such delivery systems of the

[1]*Agra Public College of Higher Education and Research Centre, Artoni, Agra, Uttar Pradesh, India 202007*
[2]*Department of Pharmacy, Indira Gandhi National Tribal University, Amarkantak, Madhya Pradesh, India 484007*
[3]*All India Institute of Medical Sciences, Bhopal, Madhya Pradesh, India 462020*

***For Correspondence:*** **sunita.minz@igntu.ac.in**

drugs necessitate the drugs being ingested multiple times daily to maintain appropriate plasma levels and realize the expected therapeutic response [2].

MET exhibits an oral bioavailability ranging from 50% to 60% when administered at doses between 500 to 1500 mg. When administered as a monotherapy, MET, a biguanide with insulin-sensitizing properties, has exhibited equivalent effectiveness to insulin or sulfonylureas in managing type 2 diabetes [3]. MET is offered in both liquid and tablet formulations and taken orally. This drug may be prescribed alone or in combination with other drugs to improve glycemic regulation [4]. As reported in the 2000 edition of the Physician's Desk Reference electronic library, food consumption has been found to lessen the extent of MET absorption and cause a minor delay in its absorption. MET is designated as a class II pharmaceutical agent, known for its high solubility and low permeability. The permeation rate limits absorption, although the drug solvation occurs swiftly. Hence, it is formulated to increase gastrointestinal transit time [5].

As a novel generation of hydrogels, multi-layered beads demonstrate enhanced physical characteristics relative to single-layered beads. Therefore, coating these beads using layer-by-layer adsorption is frequently utilized to establish a diffusion barrier, which effectively delays the swift release of drugs in meticulously controlled drug delivery systems [6]. In this case, Chitosan, Carbopol, and CMC-Na are significant polymers in bead preparation, particularly for drug delivery systems. The negatively charged carboxylate groups ($-COO^-$) on CMC-Na form electrostatic interactions with the positively charged aluminium ions ($Al^{3+}$) from $AlCl_3$. Aluminium ions ($Al^{3+}$) are multivalent, meaning they can interact with multiple carboxylate groups on different CMC chains.

This can result in cross-linking between polymer chains, potentially forming a gel or precipitate, depending on the ratio of CMC-Na to $AlCl_3$ and the pH of the solution. These interactions are often used in applications requiring gelation, such as controlled drug delivery systems or food products. Cross-linking can lead to the formation of beads or gels, which have been studied for various applications, including drug delivery systems. For instance, a study demonstrated that higher concentrations of ($AlCl_3$) (40% and 60% w/v) produced more uniform and rounded CMC-Na beads compared to lower concentrations (20% w/v). These beads were used to control the release and bioavailability of MET, indicating the potential of CMC-Na and $AlCl_3$ interactions in pharmaceutical formulations [7],[8].

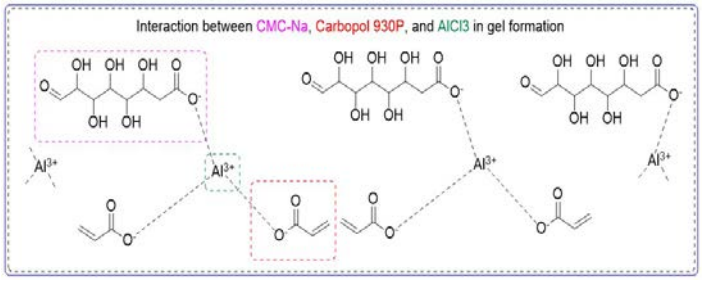


**Figure 1: The chemical interaction pattern between CMC-Na, Carbopol 934P, and Aluminium ions leads to ionotropic gelation.**

Carbopol 934P is an acrylic acid-based synthetic polymer that has been cross-linked with either polyalkenyl ethers or divinyl glycol. The interaction between Carbopol 934P (a cross-linked polyacrylic acid polymer) and aluminium chloride ($AlCl_3$) involves complex chemical dynamics influenced by multivalent metal ions. The negatively charged carboxylate groups ($-COO^-$) in Carbopol 934P interact with the positively charged aluminium ions ($Al^{3+}$) from $AlCl_3$. Carbopol polymers, including 934P, are known to interact with multivalent Metal ions such as aluminium ($Al^{3+}$). Aluminium ions ($Al^{3+}$), being trivalent, can form multiple bonds with different carboxylate groups, leading to extensive cross-linking of the Carbopol matrix.

The degree of ionization and swelling depends on the pH of the solution. The cross-linking effect of $Al^{3+}$ on Carbopol 934P can enhance its gel-forming properties, making it useful in formulations requiring high viscosity. The interaction can be exploited in drug delivery systems to form cross-linked gels that control the release of active pharmaceutical ingredients (APIs) [9], [10], [11].

Chitosan, a natural polysaccharide obtained from chitin, possesses distinctive attributes like biocompatibility, biodegradability, and reactive amino groups that facilitate surface modification and cross-linking. The chitosan coating is accomplished by electrostatic contact. Chitosan demonstrates a positive charge in acidic environments (pH < 6.5) as a result of the protonation of its amino groups ($-NH_3^+$) [12], enabling its adsorption onto negatively charged surfaces such as CMC-Na and Carbopol 934P beads through ionic interactions. The hydroxyl (-OH) groups of Chitosan enhance its hydrophilicity,

facilitating water absorption and interaction with polar molecules. The thickness of the coating and the degree of cross-linking affect the release patterns of encapsulated compounds [13], [14], [15].

Ionotropic gelation is a technique that utilizes the inherent ability of polyelectrolytes to cross-link and form hydrogel beads, known as gel spheres, when exposed to counter ions [16]. The ionotropic gelation process for fabricating beads provides several significant benefits in treating DM, particularly in improving drug delivery systems [17]. CMC-Na and carbopol are polyanionic polysaccharides characterized by a high concentration of carboxyl groups within their polymer chains, which readily facilitate the formation of hydrogels through cross-linking with $Al^{3+}$ ions [18].

In this study, hydrogel beads were first synthesized using CMC-Na and carbopol using the ionotropic gelation method. Subsequently, the prepared beads were coated with a chitosan layer, attributed to its rigid crystalline structure and minimal solubility in water and biological fluids at a pH of 7.4. MET has been recognized as a potent option in treating type 2 DM. To the best of our understanding, this represents the inaugural instance of synthesizing hydrogel beads through the introduction of CMC-Na and carbopol mixtures into an aluminum chloride solution for cross-linking, with Chitosan employed as a coating material to enhance stability and prolong release time. Various techniques were used to characterize the bilayer hydrogel beads, focusing on size, surface morphology, surface modifications, crystallinity, drug loading content, and the *in vitro* drug release profile [6].

## *MATERIALS AND METHODS*

### *Materials*

Metformin HCl was a gift sample from Yarrow Chem Products Pvt. Ltd., Mumbai. CMC-Na was acquired from CDH India, Carbopol 934P was obtained from Molychem, India, and Chitosan was procured from Himedia, Mumbai, India. All reagents and solvents employed in the experiment were of analytical grade and procured from a local supplier.

### *Preparation of Metformin-Loaded Beads*

The preparation of MET-loaded beads was accomplished through the ionotropic gelation technique. To synthesize these beads, 100 mg of MET was dissolved in a solution of CMC-Na and carbopol 934P in a specific amount. Subsequently, the drug-loaded polymeric solution was carefully injected dropwise through a syringe into different concentrations of aluminium chloride solution. The beads were left inside the aluminum chloride solution for 24 hours to determine the hardening of the beads. The beads were then filtered and thoroughly washed with distilled water, leaving them to dry in the air [19].

### *Optimization of Metformin HCl (MET) beads by Box-Behnken Design*

The optimization process for the formulations of the prepared MET beads was performed through a three-factor, two-level Box-Behnken Design (BBD) with the support of Design Expert software 8 Trial (8.0.7.1). The selected independent variables for this research included the concentrations of CMC-Na as factor A, carbopol 934P as factor B, and aluminium chloride as factor C. The response factors selected were particle size and percent drug entrapment. The design pattern can be found in Table 1.

The responses were then analyzed using statistical parameters such as the F value, $R^2$ value, p-value, lack of fit, and F value to develop an appropriate mathematical model. The model's adequacy and validity, which feature quadratic polynomial response equations alongside main and interaction factors, were analyzed through ANOVA to ascertain the best-fit model. The study focused on the dependent variables, which comprised particle size and the percent entrapment efficiency, X1 and X2, respectively. The non-linear quadratic model equation allows for the calculation of the expected X response.

**Table 1: Independent and dependent variables and their levels for Box-Behnken design used in the development of beads by ionotropic gelation technique.**

| **Variables** | | **Code levels** | | |
|---|---|---|---|---|
| **Independent variables** | | **Low (-1)** | **Medium (0)** | **High (+1)** |
| A | CMC-Na(mg) | 500 | 1000 | 1500 |
| B | CPO (mg) | 250 | 375 | 500 |
| C | $AlCl_3$ (%) | 5.00 | 7.50 | 10.0 |
| | | | | |
| **Dependent variables** | | **Goal** | | |
| X1 | Particle size(mm) | Minimum | | |
| X2 | EE (%) | Maximum | | |

**Table 2: Box-Behnken experimental design showing the outcome of different independent variables on dependent variables**

| | | Independent variables | | | Dependent variables | |
|---|---|---|---|---|---|---|
| **Std** | **Run** | **CMC-Na(mg)(A)** | **CPO (mg) (B)** | **$AlCl_3$ (%) (C)** | **Particle size (mm)** | **Entrapment Efficiency (%)** |
| 4 | 1 | 1500 | 500 | 7.50 | 184.2 | 94.4 |
| 1 | 2 | 500 | 250 | 7.50 | 204.6 | 96.42 |
| 12 | 3 | 1000 | 500 | 10.00 | 171.6 | 97.80 |
| 8 | 4 | 1500 | 375 | 10.00 | 210 | 95.93 |
| 3 | 5 | 500 | 500 | 7.50 | 153.6 | 95.32 |
| 14 | 6 | 1000 | 375 | 7.50 | 202.8 | 94.7 |
| 10 | 7 | 1000 | 500 | 5.00 | 0 | 0 |
| 7 | 8 | 500 | 375 | 10.00 | 175.8 | 97.87 |
| 5 | 9 | 500 | 375 | 5.00 | 0 | 0 |
| 13 | 10 | 1000 | 375 | 7.50 | 202.8 | 94.7 |
| 15 | 11 | 1000 | 375 | 7.50 | 202.8 | 94.7 |
| 2 | 12 | 1500 | 250 | 7.50 | 159 | 95.67 |
| 9 | 13 | 1000 | 250 | 5.00 | 0 | 0 |
| 11 | 14 | 1000 | 250 | 10.00 | 231.5 | 97.83 |
| 6 | 15 | 1500 | 375 | 5.00 | 0 | 0 |

Optimal selection was made based on desired values of response parameters like mean particle size and entrapment efficiency. Bead formulations corresponding to these optimal results were prepared and coated with Chitosan for further evaluation.

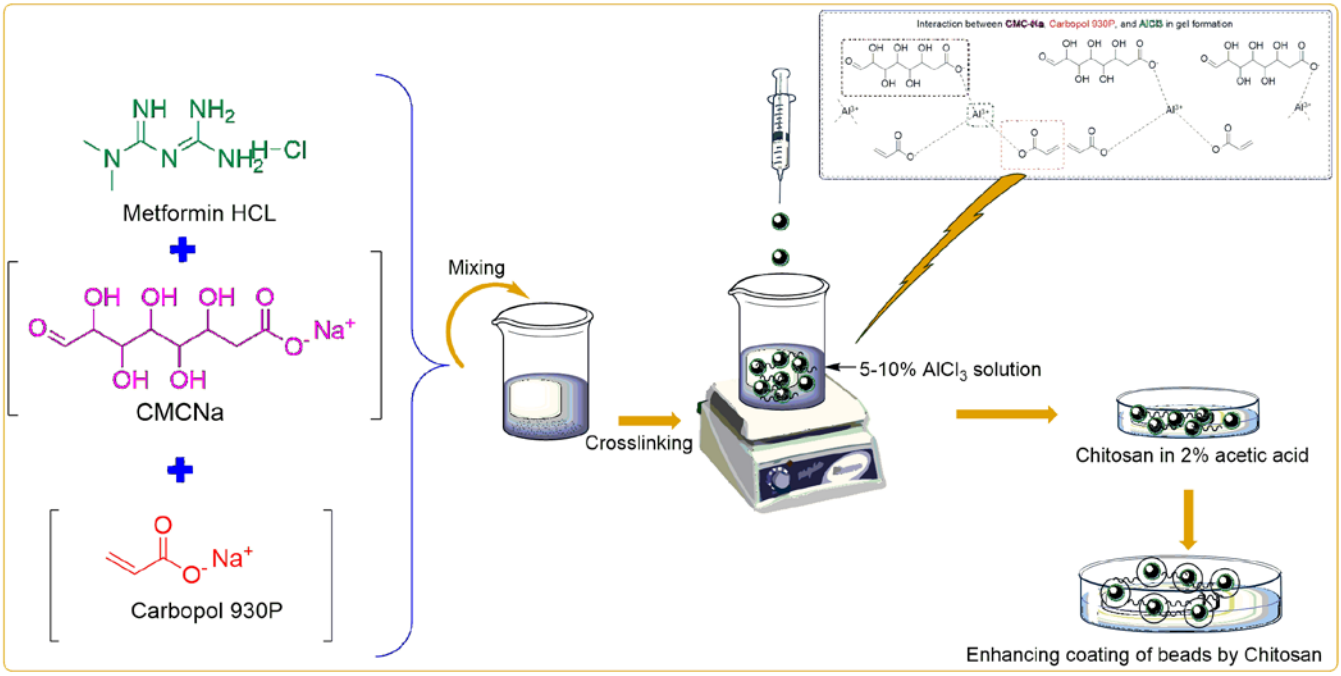


**Figure 2: The general procedure employed for preparing the chitosan-coated MET-loaded beads.**

***Coating of optimized beads with Chitosan***

2.5 grams of chitosan were dissolved in 100 milliliters of a 2% acetic acid solution to prepare the chitosan solution. The pH of this mixture was precisely adjusted to 6.0 by carefully adding 1M NaOH. The formulated beads were added to 5 mL of the chitosan solution to prepare coated beads. To enhance the coating process of beads, the suspension was mixed for 5 minutes, and beads were collected and dried at ambient temperature [20].

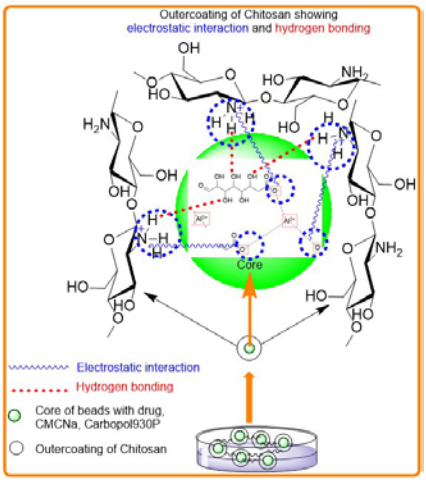


**Figure 3: Electrostatic interaction and hydrogen bonding between the -$NH_2$ group of Chitosan and the negative charge of CMC-Na and carbopol 934P.**

***Evaluation of optimized formulation***

**Percentage yield**

The percentage yield was assessed by considering the dried formulation's weight alongside the original components' total initial weight. The percentage yield can be calculated using the following equation:

$$\%\ \boldsymbol{Yield} = \frac{\boldsymbol{Practical\ Mass\ (Beads)}}{\boldsymbol{Theoritical\ mass\ (polymer + drug)}} \times \mathbf{100}$$

**Estimation of particle size**

The estimation of particle size analysis was determined using an optical microscope in conjunction with a stage micrometer slide. Around 50 beads were analyzed for particle size, and the result was recorded.

**Swelling Index**

In a simulated stomach pH of 1.2, the swelling index of beads was measured. The drug-loaded and chitosan-coated beads were each placed in separate test tubes and left to equilibrate for 8 hours at 37°C. The test tubes were removed at various intervals, and the beads were filtered before being transferred to a small beaker and weighed [19].

**Fourier transform infrared spectroscopy (FTIR)**

The FTIR spectra for both drug-loaded beads and chitosan-coated drug-loaded beads were acquired utilizing an FTIR spectrophotometer (Alpha II Eco ATR 2019-20). The beads are crushed into powder form and analyzed to determine the peaks formed for the MET-loaded and chitosan-coated MET-loaded beads in the FTIR spectrophotometer. The FTIR data was examined across the spectral region from 4000 $cm^{-1}$ to 400 $cm^{-1}$ [21].

**X-ray Diffraction (XRD)**

The crystallinity of the dried bead samples was assessed by analyzing the XRD patterns derived from composite beads, both with and without the chitosan coating, utilizing an X-ray diffractometer (Xpert3 powder Panalytical). The drug-loaded beads, encased in a chitosan coating, were reduced to a powdered state, followed by the analysis of the samples conducted within the established range of $2\Theta = 0^0$ to $90^0$ [22].

**% Entrapment efficiency**

The accurate weighing of 50 mg of each drug-loaded bead was done separately, followed by grinding and transferring into a 100 ml volumetric flask with purified water. The blend was then mixed continuously for 24 hours to attain a state of equilibrium. The polymer residue obtained after crushing the drug-loaded beads was filtered using filter paper. We could determine the drug content spectrophotometrically using the filtrate at $\lambda_{max}$ of 230 nm. Each of the experiments performed was executed three times [19].

$$\boldsymbol{EE}\ \% = \frac{\boldsymbol{Actual\ amount\ of\ drug\ present}}{\boldsymbol{Theoretical\ drug\ amount\ predicted}} \times \mathbf{100}$$

**Scanning electron microscopy (SEM)**

The morphology of the beads in the selected formulations was analyzed using SEM (COXEM-EM30). The samples were stored within the vacuum chamber and subjected to random scanning, during which photomicrographs were captured [23].

***In-vitro* drug release**

The *in-vitro* release of the drug was carried out in a phosphate buffer saline (PBS) solution with a pH of 7.4, miming intestinal fluid, employing the dialysis bag technique under sink conditions. The release studies employed a dialysis membrane with a molecular weight cutoff between 12,500 and 14,000 Daltons. The activation of the dialysis membrane was achieved by soaking it overnight in a PBS solution, which was incorporated into the release media at a pH of 7.4. Accurately measure 2 mg of MET-loaded and chitosan-coated MET-loaded beads in a dialysis bag securely tied at both ends. The dialysis bag containing the loaded beads was suspended in 100 ml of PBS at pH 7.4, with a stirring rate of 100 rpm, maintained at

37°C for 12 hours. At specified intervals, 2 ml of the dissolution medium was withdrawn through the drainage system and replaced with an equivalent volume of fresh-release media. The drug's quantity was quantified using a UV spectrophotometer, where absorbance readings were recorded at a maximum wavelength of 230 nm. All experiments were executed in triplicate to maintain reliability [16].

**Release kinetics modelling**

Several kinetic models, including first order, zero order, Korsmeyer-Peppas, Higuchi kinetics, and Hixson-Crowell models, were evaluated for the best fit of drug release data to determine the release kinetics of produced MET-loaded and chitosan-coated MET-loaded beads preparations. The optimal release kinetic model was the one that was submitted to the formulation and had the highest regression coefficient ($R^2$) [21].

## *RESULT AND DISCUSSION*

### *Optimization*

Within the framework of BBD, Design Expert 8.0.7.1 facilitated the development of 15 test formulations. Table 2 summarizes the data for these formulations' particle size and drug entrapment efficiency. Notably, the dependent variables strongly relied on the independent variables employed. Polynomial equations were used to express the results for all response variables. Furthermore, 3D graphs were utilized to depict the visual interaction of product parameters.

**Effect of formulation variables on particle size**

This model exhibits a high F-value of 128.17, signifying its significance. The occurrence of noise resulting in a substantial F-value is limited to just 0.01% of instances. According to Table 2, model expressions are considered significant when the probability value is less than 0.05, with expressions B, C, AB, BC, $A^2$, and $C^2$ crucial. Model expressions lose their meaning when values surpass 0.1000. Simplification is necessary to enhance the model if it contains numerous insignificant expressions. However, in this case, such simplification is not required since most values are below 0.100; the analysis reveals that factors A and B play a pivotal role in determining particle size, while the impact of factor C is minimal. An acceptable model necessitates an insignificant lack of fit, with the adjusted $R^2$ value of 0.9957 equating to the predicted $R^2$ value of 0.9309. The signal-to-noise ratio is measured with adequate precision, favoring ratios that exceed 4. Our determined signal-to-noise ratio of 29.012 indicates a positive result. The model can effectively guide the design space, with the resulting equation as follows:

$$Particle\ size = 202.80 + 2.40xA - 10.71xB + 98.61xC + 19.05xAB + 8.55xAC - 14.98xBC - 15.89xA^2 - 11.56xB^2 - 90.46xC^2$$

AB, AC, BC, $A^2$, $B^2$, and $C^2$ are interactive expressions that signify a non-linear relationship between responses. The particles in the formulations are measured between 153.6 mm and 231.5 mm in size. Adding a greater quantity of CMC-Na led to a notable increase in particle size, which can be explained by the accumulation during the preparation phase. This occurrence may also contribute to a more extensive particle size distribution. The result obtained after ANOVA for the quadratic model shows the significant effect of CMC-Na, Carbopol, and $AlCl_3$ on the particle size (p-value <0.0001). When the higher amount of CMC-Na and decreased carbopol in the polymer blend increased the concentration of $AlCl_3$ solution for cross-linking, the particle size significantly increased (Formulation 14). The ratio of low volume, i.e., 5% of $AlCl_3$, decreased particle size at any weight of CMC-Na and carbopol polymer. The increase in the concentration of the cross-linking agent strengthens the connections within the polymer network, thereby facilitating the formation of larger entities. These more stable beads are less prone to break. Particle size increases due to the beads' increased viscosity, swelling, and gelation rate.

**% Entrapment efficiency**

The design expert established the model's significance through the 13495.65 F-value. The expected $R^2$ of 0.9999 corresponds effectively with the modified $R^2$ of 0.9993. The polynomial equation derived for this model is as stated:

$$\%\ Entrapment\ Efficacy = 94.70 - 0.45xA - 0.30xB + 48.68xC - 0.042xAB - 0.49xAC - 7500E - 003xBC + 0.15xA^2 + 0.61xB^2 - 46.40xC^2$$

All batches exhibited an entrapment efficiency ranging from 90.88% to 95.55% (as shown in Table 1). The data indicated that the %EE percentage of the MET-containing beads increased with the elevation of CMC-Na and a reduction in carbopol content in the polymer blend, in conjunction with an increase in the concentration of the $AlCl_3$ solution. Porous structures can also result from an imbalance in the ionic interaction (CMC-Na and carbopol) or cross-linking agent ($AlCl_3$), which lowers the drug's retention capacity. Enhancing drug retention in the bead matrix and maximizing formulation performance requires understanding these formulation-dependent mechanisms (such

as PEE and particle size). The observed increase in PEE (%) with the addition of more CMC-Na in these beads could be explained by the rising viscosity of the polymer (CMC-Na) solution that occurs with higher polymer concentrations; such an approach may have served to prevent the migration of drugs into the cross-linking solution.

Additionally, the augmented presence of CMC-Na within the polymer blend could have intensified the cross-linking process induced by $AlCl_3$ by offering increased sites for ionic interactions. In evaluating the fifteen batches, fourteen achieved a remarkable drug entrapment efficiency of 97.8%. The observed result could be attributed to the elevated levels of CMC-Na and the maximum concentration of $AlCl_3$ at 10%, which enhances the drug's entrapment relative to formulation 13, which features a reduced amount of carbopol, 5% $AlCl_3$, and an absence of CMC-Na.

**Optimization and validation of the BBD outcomes**

The formulation of MET beads was precisely determined, considering aspects like particle size and entrapment efficiency. Identifying independent factors was achieved through statistical analysis and graphical representation, focusing on the intended response values. After applying the BBD experimental design for point prediction, an optimized formulation of MET-loaded beads was chosen based on desirability factors. The response variables of the experimental batch, developed and characterized using the projected independent factors, were thoroughly examined. The anticipated and achieved outcomes, precisely an average particle size of 188.12 mm and an encapsulation efficiency of 95.94%, are in substantial agreement, thereby validating the effectiveness of the optimized MET bead formulation.

***% yield***

The optimized formulations exhibited a percentage yield of 98.4%. Higher entrapment efficiency reveals that CMC and Carbopol are polymers with functional groups (like carboxyl groups) that can interact with MET through hydrogen bonding, electrostatic forces, or other molecular interactions.

These interactions help the drug more effectively encapsulate within the polymer matrix, leading to higher entrapment efficiency. CMC and Carbopol are hydrophili**c** polymers with a strong affinity for water. MET, which is water-soluble, is efficiently incorporated into the hydrophilic network of these polymers, as the polymers can easily swell in water, providing a suitable environment for the drug to be imprisoned.

***Swelling index***

The investigation of swelling *in vitro* was conducted under pH 1.2 at a temperature of 37°C, and the gravimetric determination was used to measure the degree of swelling (wt.%) for each sample. The formulation's swelling index was higher in drug-loaded beads than in chitosan-coated beads. The drug itself may be hydrophilic or have qualities that encourage water absorption, leading the drug-loaded beads to grow more during the swelling test as they absorb water. When exposed to water, Chitosan can produce a hydrogel-like structure, contributing to more significant swelling. The chitosan coating may form a hydrogel layer on the beads, increasing water absorption and swelling. Combining chitosan, drug, and bead matrix features may result in a distinct swelling behavior in chitosan-coated MET-loaded beads, resulting in a more significant swelling.

***FTIR***

Figure 5 compares FTIR spectra of MET, MET-loaded beads, and chitosan-coated MET-loaded beads, respectively. Corresponding IR peaks to N-H stretching secondary and primary amine vibrations, respectively. The FTIR spectra of MET showed distinctive peaks at around 3360-3370 $cm^{-1}$ and 3290-3300 $cm^{-1}$. The C=N stretching of the imine group was identified as the cause of a clear peak close to 1625-1650 $cm^{-1}$. Peak values between 1550 and 1570 $cm^{-1}$ also showed N-H bending; those between 1470 and 1490 $cm^{-1}$ and 1020–1040 $cm^{-1}$ were given C-N stretching vibrations. These unique peaks verify the existence of functional groups compatible with the chemical composition of MET [24]. The distinctive spectral peaks associated with MET functional groups were observed in both optimized samples (A) MET-loaded beads and (B) Chitosan-coated MET-loaded beads, indicating that MET and excipients such as CMC-Na, in the context of bead design and development via the ionotropic gelation method, Carbopol and Chitosan, exhibited compatibility. All the above-observed peaks of FT-IR indicate the presence of all necessary peaks of MET in Chitosan-coated MET-loaded beads.

***XRD***

XRD serves as a valuable resource in studying the crystal lattice arrangement, offering a wealth of helpful information about the

crystallinity of the sample. The prominent semicrystalline feature of Chitosan is fundamentally linked to the significant quantity of amino and hydroxyl groups incorporated into its composition. These groups can form strong inter- and intramolecular hydrogen bonds, contributing to the overall crystalline behavior. The broad peaks in the XRD diffractogram demonstrate that incorporating chitosan coating on MET-loaded beads effectively mitigated polymer crystallization. In contrast, the graph illustrates the amorphous nature of the bead's formulation in drug-loaded beads (Figures 6 & 7).

***Surface Morphology***

In Figure 8, images show the bead structure and surface morphology of the MET-loaded beads and chitosan-coated MET-loaded beads. The irregularity suggests a higher polymer concentration on the beads' surface. Surface morphology is also observed under the microscope, determining the spherical structure of the beads. In Figure 8, the MET-loaded beads have a rough surface on the outer coating, while in the chitosan-coated beads, the outer layers of the beads are covered with the chitosan layer, which indicates that the coating is done on the beads. The drug-loaded beads have a spiral outer layer, which can be easily identified in the SEM image of the MET-loaded beads mentioned in sections a and b. In sections c and d of the figure, the rough surface is covered with a layer that can be distinguished as the chitosan coating on the chitosan-coated MET-loaded beads.

***In-vitro release study***

An assessment of the *in vitro* release profile of MET was conducted over a 10-hour timeframe at pH 7.4, employing a release medium maintained at pH 1.2. All studies were done in triplicate. Specifically, after 30 minutes, 32.9% of the drug was released from the drug-loaded beads, whereas the chitosan-coated drug-loaded beads released 26.1%. After 10 hours, the total drug release from the beads containing the drug was measured at 55.5%, in contrast to the 48.8% release observed from the chitosan-coated drug-loaded beads (Figure 9). The in vitro drug release profile revealed a continuous release of MET throughout 10 hours from both MET-loaded and chitosan-coated MET-loaded beads.

Over the first two hours, there was an initial burst release, then a slow, steady release. At all times, MET-loaded beads showed a larger cumulative drug release than chitosan-coated beads. The chitosan coating probably slowed down drug diffusion using its barrier-forming characteristics, which can control the release rate. This suggests that chitosan coating helps to create a more regulated release profile, therefore improving the fit of the formulation for long-term drug administration.

**Table 3: Summary of ANOVA for the response parameters in Box-Behnken experimental design.**

| Source | Particle size (mm) | | Entrapment Efficiency (%) | |
|---|---|---|---|---|
| | Sum of squares | p-value | Sum of squares | p-value |
| Model | 1.120E+005 | <0.0001 | 27017.14 | <0.0001 |
| A-CMC | 46.08 | <0.0001 | 1.63 | 0.0425 |
| B-CPO | 918.06 | 0.5215 | 0.72 | 0.1319 |
| C-$AlCl_3$ | 77795.40 | 0.0276 | 18956.97 | <0.001 |
| AB | 1451.61 | <0.001 | 7.225E-0.003 | 0.8641 |
| AC | 292.41 | 0.0118 | 0.94 | 0.0948 |
| BC | 897.00 | 0.1431 | 2.250E-004 | 0.9759 |
| $A^2$ | 931.99 | 0.0288 | 0.080 | 0.5741 |
| $B^2$ | 493.63 | 0.0269 | 1.35 | 0.0569 |
| $C^2$ | 30215.87 | 0.0738 | 7948.53 | <0.0001 |
| Residual | 485.63 (sum of square) | | 1.11 (sum of square) | |
| Lack of fit | Not significant | | Not Significant | |
| Pure error | 0.000 | | 0.000 | |
| $R^2$ | 0.9357 | | 0.999 | |
| Predicted $R^2$ | 0.9309 | | 0.9999 | |
| Adjusted $R^2$ | 0.9879 | | 0.9993 | |

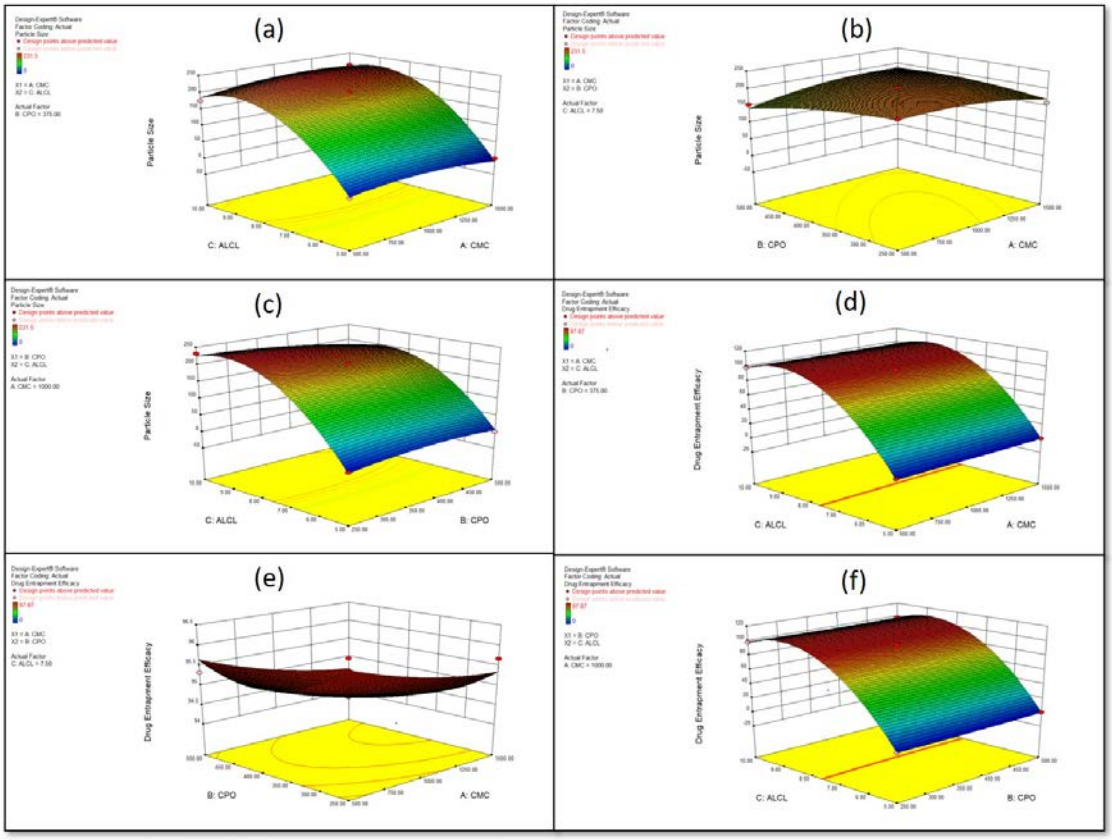


**Figure 4: The surface response 3D plot showing (a) the CMC-Na amount and the $AlCl_3$% ratio influence on particle size. (b) The influence of CPO amount and CMC-Na on Particle size. (c) The influence of $AlCl_3$% and CPO ratio on Particle size. (d) The influence of CMC-Na amount and $AlCl_3$% ratio on EE. (e) The influence of CPO amount and CMC-Na on EE. (f) The influence $AlCl_3$% and CPO ratio on EE.**

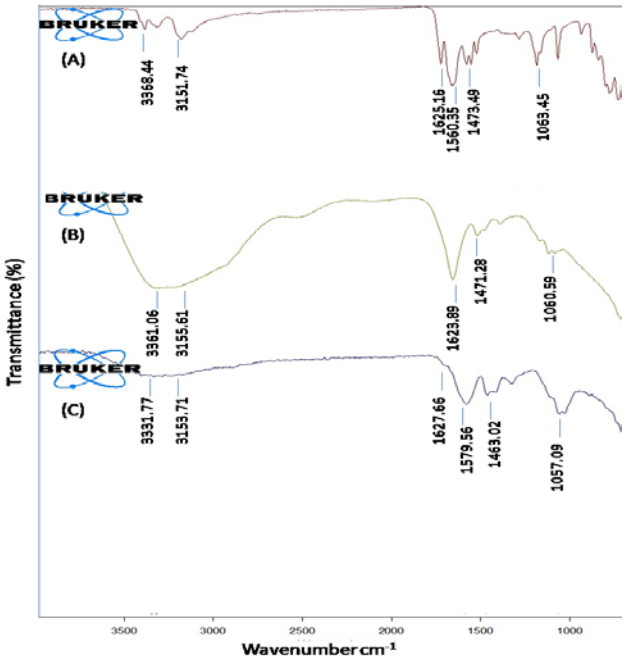


**Figure 5: FTIR graph of (A) MET (B) MET-loaded beads (C) Chitosan-coated MET-loaded beads**

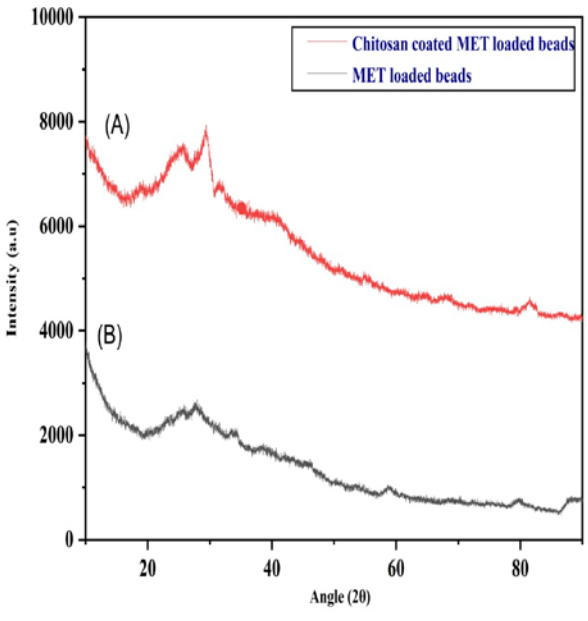


**Figure 6: X-ray diffractogram of (A) chitosan-coated MET-loaded beads and (B) MET-loaded beads**

***Release Kinetics Modelling***

Several kinetic equations were employed to assess the release data to characterize drug release kinetics from beads. The analysis of the data was performed using the regression coefficient technique. The regression coefficient ($R^2$) values illustrated in Figures 10 and 11 were derived using the least-squares technique, ensuring a confidence level of 95%. The evaluation of the regression coefficient values across all formulations demonstrated that both the MET-loaded beads and the chitosan-coated MET-loaded beads aligned with the Korsmeyer-Peppas model, achieving the most significant regression ($R^2$) values of nearly 0.958 and 0.946. Data analysis aligned with the Korsmeyer-Peppas equation demonstrated that the drug release was facilitated by a diffusion process that displayed non-Fickian behavior. Further investigation of the release data indicates that the formulations (i.e., MET-loaded beads and the chitosan-coated MET-loaded beads) fit well within the Korsmeyer-Peppas model. The Higuchi model is the second-best-fitted model compared to the other two kinetic models. In the context of the Higuchi model, the MET-loaded beads and chitosan-coated MET-loaded beads demonstrated $R^2$ values of 0.745 and 0.826, respectively, suggesting that the release process occurs predominantly through diffusion.

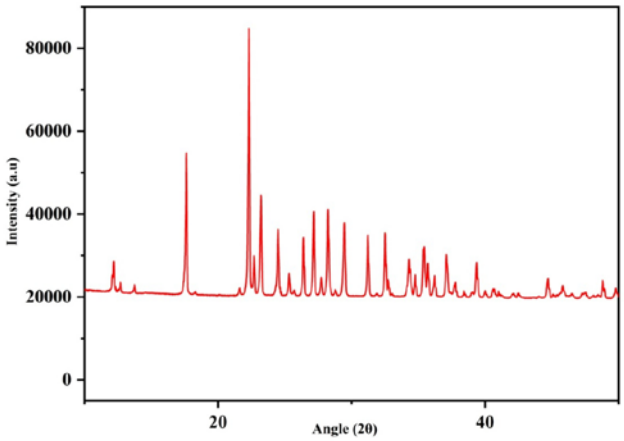


**Figure 7: X-ray diffractogram of MET**

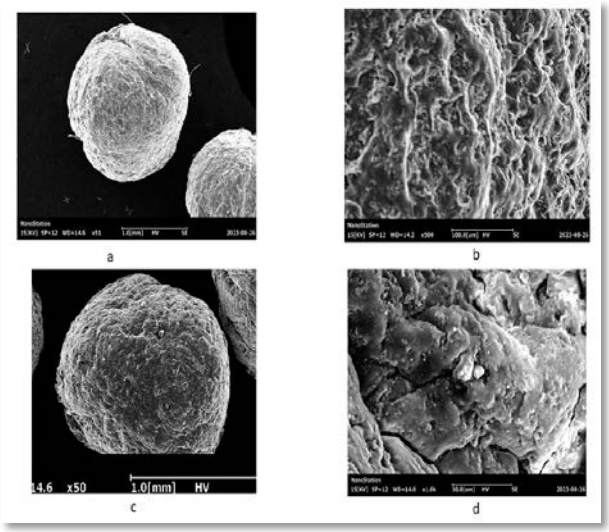


**Figure 8: SEM images (a) and (b) of MET-loaded beads, (c) and (d) of chitosan-coated MET-loaded beads**

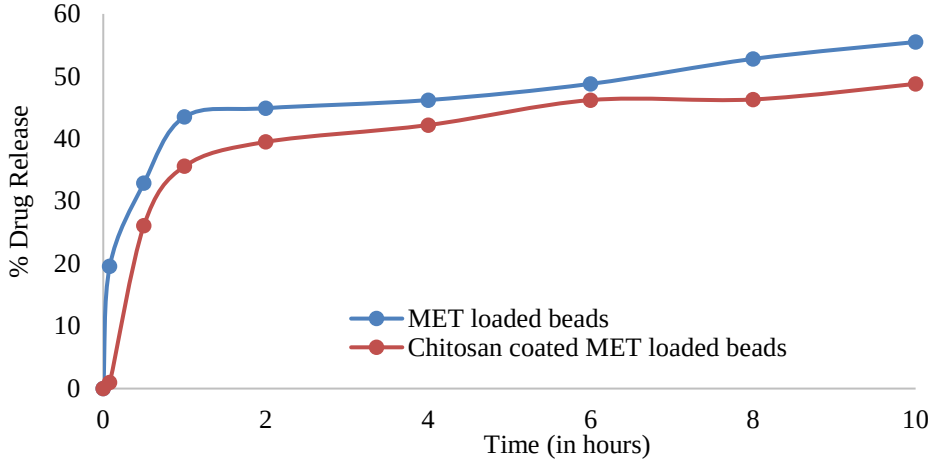


**Figure 9: *In-vitro* cumulative percentage release of MET-loaded beads and chitosan-coated MET-loaded beads**

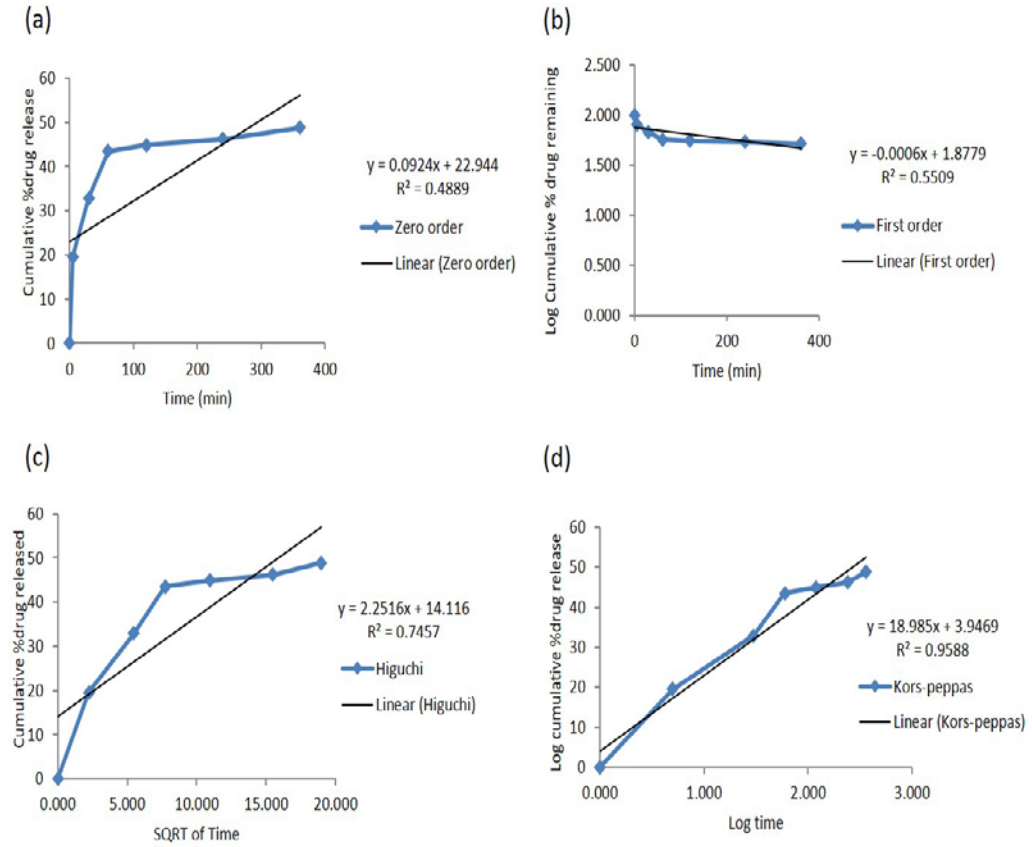


**Figure 10: Drug release data fitted to various kinetic models: (a) Zero order (b) First order (c) Higuchi model (d) Korsmeyer-Peppas (Kors-Peppas) of MET loaded beads in 7.4 pH buffer.**

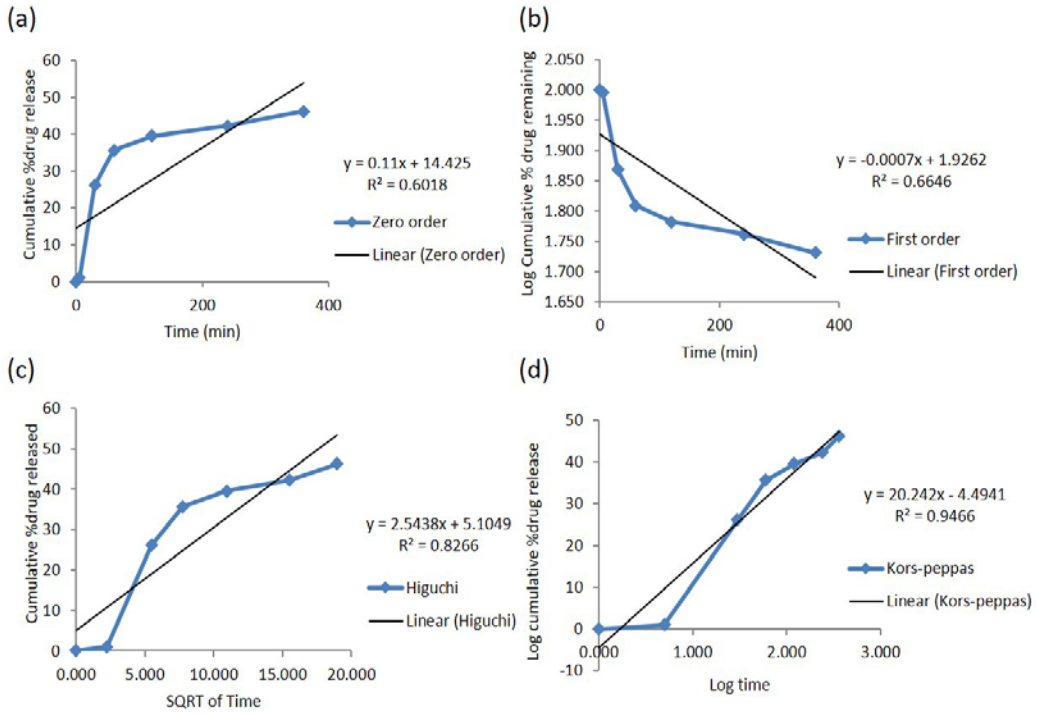


**Figure 11: Drug release data fitted to various kinetic models: (a) Zero order model (b) First order model (c) Higuchi model (d) Korsmeyer-Peppas (Kors-Peppas) model of Chitosan-coated MET-loaded beads in 7.4 pH buffer.**

## *CONCLUSION*

As carbopol is insoluble in low pH 1.2 and tends to form a gel-like structure, this gel formation can make the carbopol appear more swell, but it does not fully dissolve. As a result of this enlargement, pore formation occurs, and drug release from the matrix occurs more slowly. This polymer-based matrix system (carbopol and CMC-Na) is loaded with MET and coated with the polymer chitosan to regulate the release rate. The presence of an amine group in its structure renders Chitosan a polymer with a positive charge. When this matrix system is coated, the MET is released when the matrix swells and degrades over time.

## *ACKNOWLEDGMENTS*

The authors are grateful to Kalinga University, Raipur, for the Scanning Electron Microscopy facility. They also gratefully acknowledge the Department of Pharmacy, Indira Gandhi National Tribal University, Amarkantak, for providing FTIR CIF and basic lab facilities, and the Department of Chemistry, Indira Gandhi National Tribal University, Amarkantak, for the XRD facility.

## *FINANCIAL ASSISTANCE*

Nil

## *CONFLICT OF INTEREST*

The authors declare no conflict of interest in this manuscript.

## *AUTHORS CONTRIBUTION*

Sachin Gupta designed the study methodology and wrote the original draft; Swati Dubey and Sanjeev Kumar Patel contributed by writing, reviewing, and editing the original draft; Anshu Priyanka Lakra contributed to data conceptualization, software, and formal analysis; Sunita Minz contributed by Supervising, Resources, Project, Methodology, Investigation, and Conceptualization and edited the manuscript for clarity and grammar.

## *REFERENCES*

[1] Tentolouris A, Vlachakis P, Tzeravini E, Eleftheriadou I, Tentolouris N. SGLT2 inhibitors: A review of their antidiabetic and cardioprotective effects. *Int J Environ Res Public Health*, **16**, 1–27 (2019) https://doi.org/10.3390/ijerph16162965.

[2] M A, Gogate PR. Improved synthesis of metformin hydrochloride-sodium alginate (MH-NaALG) microspheres using ultrasonic spray drying. *Heliyon*, **10**, e28205 (2024) https://doi.org/10.1016/j.heliyon.2024.e28205.

[3] Kirpichnikov D, McFarlane SI, Sowers JR. Metformin: An Update. *Ann Intern Med*, **137**, 25–33 (2002) https://doi.org/10.7326/0003-4819-137-1-200207020-00009.

[4] Kurdi A, Alhussaini W, Alawaji A, Alhudathi A, Alharbi R, Binsaleh F, Alghamidi Y, Al Bekairy A, Alkatheri A, Islam I, Farh I, Ghanem E, Mansour M. Comparative performance of liquid chromatography and spectrophotometry in determining metformin hydrochloride within pharmaceutical formulations. *Heliyon*, **10**, e32551 (2024) https://doi.org/10.1016/j.heliyon.2024.e32551.

[5] Ozoude CH, Azubuike CP, Ologunagba MO, Tonuewa SS, Igwilo CI. Formulation and development of metformin-loaded microspheres using Khaya senegalensis (Meliaceae) gum as co-polymer. *Futur J Pharm Sci*, **6**, (2020) https://doi.org/10.1186/s43094-020-00139-6.

[6] Karzar Jeddi M, Mahkam M. Magnetic nano carboxymethyl cellulose-alginate/chitosan hydrogel beads as biodegradable devices for controlled drug delivery. *Int J Biol Macromol*, **135**, 829–38 (2019) https://doi.org/10.1016/j.ijbiomac.2019.05.210.

[7] Hosny EA, Al-Helw AA-RM. Effect of coating of aluminum carboxymethylcellulose beads on the release and bioavailability of diclofenac sodium. *Pharm Acta Helv*, **72**, 255–61 (1998) https://doi.org/10.1016/S0031-6865(97)00040-X.

[8] Lopez CG, Colby RH, Cabral JT. Electrostatic and Hydrophobic Interactions in NaCMC Aqueous Solutions: Effect of Degree of Substitution. *Macromolecules*, **51**, 3165–75 (2018) https://doi.org/10.1021/acs.macromol.8b00178.

[9] Zakzak K, Semenescu AD, Moacă EA, Predescu I, Drăghici G, Vlaia L, Vlaia V, Borcan F, Dehelean CA. Comprehensive Biosafety Profile of Carbomer-Based Hydrogel Formulations Incorporating Phosphorus Derivatives. *Gels*, **10**, (2024) https://doi.org/10.3390/gels10070477.

[10] López-Cacho JM, González-R PL, Talero B, Rabasco AM, González-Rodrguez ML. Robust optimization of alginate-Carbopol 940 bead formulations. *The Scientific World Journal*, 2012, (2012) https://doi.org/10.1100/2012/605610.

[11] Mahmood A, Mahmood A, Ibrahim MA, Hussain Z, Ashraf MU, Salem-Bekhit MM, Elbagory I. Development and Evaluation of Sodium Alginate/Carbopol 934P-Co-Poly (Methacrylate) Hydrogels for Localized Drug Delivery. *Polymers (Basel)*, **15**, (2023) https://doi.org/10.3390/polym15020311.

[12] de Souza HKS, Bai G, Gonçalves M do P, Bastos M. Whey protein isolate–chitosan interactions: A calorimetric and spectroscopy study. *Thermochim Acta*, **495**, 108–14 (2009) https://doi.org/10.1016/j.tca.2009.06.008.

[13] Zhao D, Shen X. Preparation of Chitosan-Diatomite/Calcium Alginate Composite Hydrogel Beads for the Adsorption of Congo Red Dye. *Water (Switzerland)*, **15**, (2023) https://doi.org/10.3390/w15122254.

[14] Fatullayeva S, Tagiyev D, Zeynalov N, Mammadova S, Aliyeva E. Recent advances of chitosan-based polymers in biomedical applications and environmental protection. *Journal of Polymer Research*, **29**, 259 (2022) https://doi.org/10.1007/s10965-022-03121-3.

[15] Zia Q, Tabassum M, Gong H, Li J. A Review on Chitosan for the Removal of Heavy Metals Ions. *Journal of Fiber Bioengineering and Informatics*, **12**, 103–28 (2019) https://doi.org/10.3993/jfbim00301.

[16] Essifi K, Lakrat M, Berraaouan D, Fauconnier ML, El Bachiri A, Tahani A. Optimization of gallic acid encapsulation in calcium alginate microbeads using Box-Behnken Experimental Design. *Polymer Bulletin*, **78**, 5789–814 (2021) https://doi.org/10.1007/s00289-020-03397-9.

[17] Gadziński P, Froelich A, Jadach B, Wojtyłko M, Tatarek A, Białek A, Krysztofiak J, Gackowski M, Otto F, Osmałek T. Ionotropic Gelation and Chemical Crosslinking as Methods for Fabrication of Modified-Release Gellan Gum-Based Drug Delivery Systems. *Pharmaceutics*, **15**, 108 (2022) https://doi.org/10.3390/pharmaceutics15010108.

[18] Hu Y, Hu S, Zhang S, Dong S, Hu J, Kang L, Yang X. A double-layer hydrogel based on alginate-carboxymethyl cellulose and synthetic polymer as sustained drug delivery system. *Sci Rep*, **11**, 1–14 (2021) https://doi.org/10.1038/s41598-021-88503-1.

[19] Komati S, Swain S, Rao MEB, Jena BR, Dasi V. Mucoadhesive multiparticulate drug delivery systems: An extensive review of patents. *Adv Pharm Bull*, **9**, 521–38 (2019) https://doi.org/10.15171/apb.2019.062.

[20] Nualkaekul S, Lenton D, Cook MT, Khutoryanskiy V V., Charalampopoulos D. Chitosan coated alginate beads for the survival of microencapsulated Lactobacillus plantarum in pomegranate juice. *Carbohydr Polym*, **90**, 1281–7 (2012) https://doi.org/10.1016/j.carbpol.2012.06.073.

[21] Deepak P, Kumar P, Arya DK, Pandey P, Kumar S, Parida BP, Narayan G, Singh S, Rajinikanth PS. c(RGDfK) anchored surface manipulated liposome for tumor-targeted tyrosine kinase inhibitor (TKI) delivery to potentiate liver anticancer activity. *Int J Pharm*, **642**, 123160 (2023) https://doi.org/10.1016/j.ijpharm.2023.123160.

[22] Aggarwal G, Nagpal M. Pharmaceutical Polymer Gels in Drug Delivery. *Polymer Gels: Perspectives and Applications*. (Thakur Vijay Kumar and Thakur Manju Kumari and Voicu Stefan Ioan ed.), Springer Singapore, Singapore, pp. 249–84 (2018) https://doi.org/10.1007/978-981-10-6080-9_10

[23] Altam AA, Zhu L, Huang W, Huang H, Yang S. Polyelectrolyte complex beads of carboxymethylcellulose and chitosan: The controlled formation and improved properties. *Carbohydrate Polymer Technologies and Applications*, **2**, 100100 (2021) https://doi.org/10.1016/j.carpta.2021.100100.

[24] Sabbagh BA, Kumar PV, Chew YL, Chin JH, Akowuah GA. Determination of metformin in fixed-dose combination tablets by ATR-FTIR spectroscopy. *Chemical Data Collections*, 39, 100868 (2022) https://doi.org/10.1016/j.cdc.2022.100868.